phys. stat. sol. (c) **4**, No. 10, 3646–3649 (2007) / **DOI** 10.1002/pssc.200775793

Ion species dependence of the implantation-induced defects in ZnO studied by a slow positron beam

Z. Q. Chen*[1], **M. Maekawa**[2], **A. Kawasuso**[2], and **H. Naramoto**[2]

[1] Department of Physics, Wuhan University, Wuhan 430072, P. R. China
[2] Advanced Science Research Center, Japan Atomic Energy Agency, 1233 Watanuki, Takasaki, Gunma 370-1292, Japan

Received 23 July 2006, accepted 15 June 2007
Published online 13 August 2007

PACS 61.72.Ji, 61.80.Jh, 78.70.Bj

In this work, we implanted B^+, O^+, Al^+, and P^+ ions into ZnO with energy of 50-380 keV and total doses of 4×10^{15} cm $^{-2}$ for each ion. The implantation-induced defects and their thermal recovery were studied using a slow positron beam. Vacancy clusters are produced in all the implanted samples. It is found that the thermal recovery of these vacancies induced by different ions shows much difference. In case of B^+ and Al^+-implantation, the vacancy clusters agglomerate to much larger size and might evolve to microvoids during annealing. However, for O^+ and P^+ ions, which are heavier than B^+ and Al^+, the vacancies show a much weaker agglomeration process. The mechanism of such difference is discussed.

© 2007 WILEY-VCH Verlag GmbH & Co. KGaA, Weinheim

1 Introduction Zinc oxide (ZnO) is a technologically very important semiconductor for the potential application in short wavelength light emitting devices [1]. This is due to its wide band gap (3.4 eV) and large exciton binding energy (60 meV). It has been revealed that ZnO has high resistance to electron radiation [2] due to the efficient dynamic annealing of the defects. Recently an unusual behavior related to the implantation damage in ZnO was also reported. That is the chemical effect of the damage accumulation [3]. The implantation-induced defects can be stabilized by the implanted impurities, and enhance damage buildup or even cause amorphization effects.

In this paper, we implanted several ion species into ZnO, and studied the implantation-induced defects using a slow positron beam. Our results show that the thermal recovery of implantation-induced defects is dependent of the ion species, which might be due to the chemical effects of the ions.

2 Experiment The samples are hydrothermally grown ZnO single crystals from the Scientific Production Company nominally undoped with n-type conductivity. Ion implantation was carried out at room temperature using a 400 keV implanter. A multi-step implantation process was performed for each ion with seven different energies. The energy range was 40-300 keV for B^+ and 50–380 keV for other three ions with a stepwise increase of energy during implantation, and the total doses were about $4\text{-}5\times10^{15}$ cm^{-2}. By choosing appropriate dose for each energy, a box-shaped implantation profile is obtained. The implanted samples were annealed isochronally from 200 to 1100 °C for 30 min in nitrogen ambient.

Doppler broadening of positron annihilation radiation was measured using a slow positron beam (0.2–30 keV). The S parameter defined as the ratio of the counts in the central region to the total area of the annihilation peak was used to characterize the spectrum. Micro-Raman scattering measurements were performed using the NANOFINDER spectrometer in the wave number range of 200-800 cm^{-1}. The 488.0 nm-line of an Ar^+-ion laser was used for excitation and the incident laser power was $\sim$1 mW.

* Corresponding author: e-mail: chenzq@whu.edu.cn, Phone: +86 27 6875 2370, Fax: +86 27 6875 3880

WILEY InterScience® DISCOVER SOMETHING GREAT

© 2007 WILEY-VCH Verlag GmbH & Co. KGaA, Weinheim

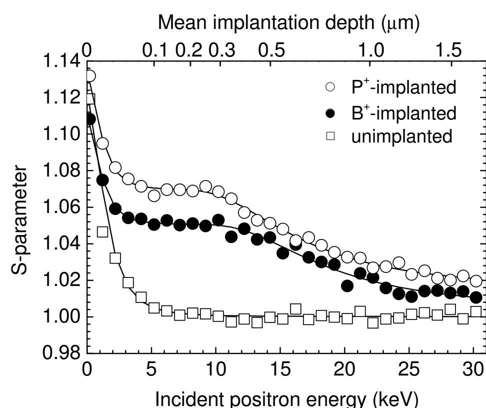

Fig. 1 S-E curves measured for ZnO samples before and after B^+ and P^+-implantation. The S–E curves for O^+ and Al^+-implanted sample are similar, so they are not presented in the figure.

3 Results and discussion Figure 1 shows the S parameter as a function of incident positron energy (S–E curve) for the as-grown and implanted samples by B^+ and P^+ ions. The S–E curves for the O^+ and Al^+-implanted sample are not shown in the figure, as they are similar to that of B^+ and P^+-implanted one, respectively. The S parameters are normalized to the value in the as-grown sample which contains no or very few defects [4]. An increase of the S parameter can be observed after implantation, which shows introduction of vacancy defects. The S parameter in the positron energy range of 5–11 keV is nearly constant, which corresponds to the box-shaped implantation layer. The S value of 1.05–1.07 suggests that implantation produces mostly vacancy clusters. Some monovacancies may also have been produced and coexist with vacancy clusters.

Figure 2 shows the average S parameter in the implanted layer (positron energy of about 5–10 keV) as a function of annealing temperature for all the implanted samples. It can be observed that the annealing behavior shows much difference for different ion implantation. As shown in Fig. 2(a), for the O^+-implanted ZnO, the S parameter first increases up to about 1.08 at 400 °C, and then decreases rapidly with increasing annealing temperature. The increase of S parameter suggests mostly the agglomeration of vacancies into larger size. After further annealing at high temperatures, these vacancy clusters are no longer stable, and they gradually recover. At 700–800 °C, the S parameter decreases to the bulk value, suggesting full recovery of these vacancies.

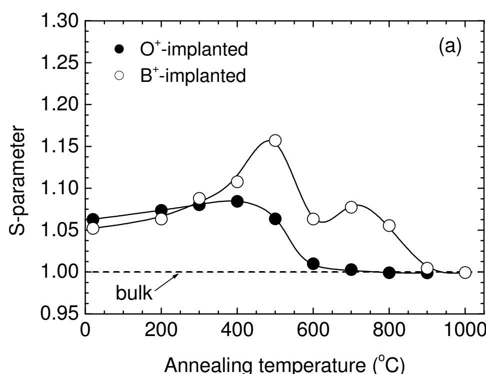

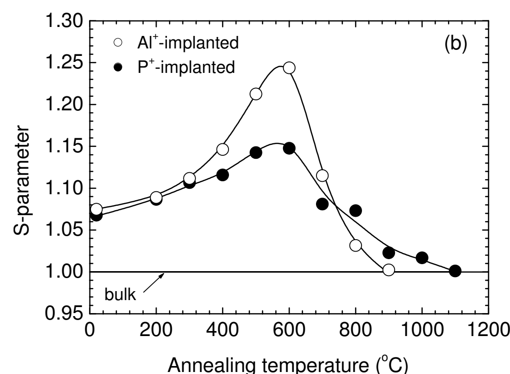

Fig. 2 Average S parameter in the implanted layer as a function of annealing temperature.

For the B^+-implanted sample, the annealing behavior of vacancies is similar. However, the S parameter increases to a high value of nearly 1.16 after annealing at 500 °C. This means that much larger vacancy clusters or microvoids are formed. After annealing at 600 °C, the S parameter begins to decrease. However, it shows a small increase again at 700 °C, and after that, it decreases gradually to the bulk value at 900–1000 °C, which indicates annealing out of the vacancy defects introduced by implantation.

© 2007 WILEY-VCH Verlag GmbH & Co. KGaA, Weinheim

The B^+ ion has a much smaller ion mass than that of O^+ ion, and the energy for B^+ ion is also lower, therefore, the vacancy concentration produced by O^+-implantation should be higher. Our TRIM simulation indeed shows that the average vacancy concentration produced by O^+-implantation in the box-layer is about 7×10^{22} cm^{-3}, while it is 4×10^{22} cm^{-3} for B^+-implantation. Despite a higher vacancy concentration in the O^+-implanted sample, the S parameter shows very slight increase after annealing, suggesting that further agglomeration of the vacancy clusters is very weak. On the contrary, for the B^+-implanted sample, the vacancy clusters grow into very large size during annealing. This suggests that boron might have special chemical effect that favors the agglomeration of vacancy clusters.

The similar difference can be observed in Fig. 2(b) for the Al^+ and P^+-implanted samples. For the Al^+-implanted sample, the S parameters increase to as high as 1.25 after annealing at 600°C, indicating that microvoids are formed due to vacancy agglomeration. However, for the sample implanted by the heavier P ions, the S parameters increase only to about 1.15. This means a much lower concentration of microvoids or smaller size of vacancy clusters. In other words, the Al^+ may also has chemical effect on defects.

Figure 3 shows the Raman spectra measured for all the implanted samples. In the as-grown ZnO, there are three phonon modes: E_2 at 437 cm^{-1}, a small peak at 575 cm^{-1}, and a multi-phonon mode at 331 cm^{-1}. After implantation, the peak at 575 cm^{-1} becomes high and broad. This is apparently due to the implantation-induced damage, which breaks the Raman selection rule, and many other phonon modes that are forbidden in the perfect lattice participate in the Raman spectrum, thus contribute to the broad peak at 575 cm^{-1}. This phonon mode has been attributed to the oxygen vacancy (V_O) since it also appears in the ZnO grown under oxygen deficient condition [5]. We have observed the same broad peak in electron-irradiated ZnO [4], and found its recovery at around 400 °C, which coincides with that of oxygen vacancies [6]. Thus it confirms that the broad peak at 575 cm^{-1} is related to V_O.

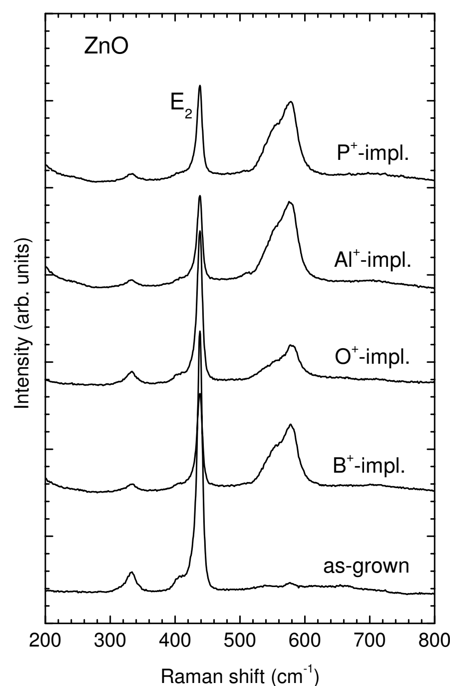

Fig. 3 Raman spectra of ZnO measured before and after ion-implantation.

Figure 4 shows the relative intensity of the 575 cm^{-1} peak for the implanted samples as a function of annealing temperature. Before annealing, the broad peak intensity of the O^+-implanted sample is the lowest, while that of the Al^+-implanted one is the highest. With increasing annealing temperature, the broad peak in all the implanted samples decreases gradually. Their annealing processes also show differences. As shown in Fig. 4, in the O^+-implanted sample, the broad peak decreases rapidly and reaches the same level as the unimplanted state after annealing at 400 °C. This means that V_O disappears early at 400 °C. While for the B^+-implanted sample, the broad peak remains high intensity until annealing at 700 °C, indicating that V_O has much higher thermal stability. A comparison between Al^+ and P^+-implantation also reveals that the broad peak intensity is always higher in the Al^+-implanted sample during annealing.

The agglomeration of vacancy clusters involves combining small vacancies like monovacancies (V_{Zn} and V_O), so that the size of the vacancy cluster increases. This means that V_O has a contribution to the vacancy cluster agglomeration. In the O^+-implanted sample, the number of V_O is much smaller compared with other implanted samples, and they disappear rapidly after annealing, therefore their contribution to

© 2007 WILEY-VCH Verlag GmbH & Co. KGaA, Weinheim

the vacancy cluster growth is also small. This might be the reason for the slight increase of S parameter after annealing. For the B^+-implanted sample, it introduces much higher concentration of V_O, and they are stable up to 700 °C, thus the vacancy cluster can grow into a sufficiently large size. The number of V_O produced by Al^+-implantation is also higher than that produced by P^+-implantation, so that large number of microvoids are formed after annealing the Al^+-implanted sample. This may well explain the positron annihilation results.

The chemical effect of B^+ and Al^+ ions is thus due to the stabilization of V_O. The boron impurity might trap O_i produced by implantation, and form oxide complexes like B_2O_3. Since the B_2O_3 compound has a much lower enthalpy of formation (–1273.5 kJ/mol) than that of ZnO (–350.5 kJ/mol) [7], the formation of such complex is very likely. In the Al^+-implanted sample, the Al_2O_3 complexes may also have been formed, as it has even lower enthalpy of formation (–1675.7 kJ/mol). Due to these complex formation, the recombination between V_O and O_i is suppressed, so the oxygen vacancies are stabilized, and they are likely to contribute to the formation of large vacancy clusters or microvoids through agglomeration. While for O^+-implantation, as it is a self-atom in ZnO, there is no complex formation with O_i. On the contrary, the O^+-implantation produces large amounts of oxygen interstitials, which expedite the recombination of V_O with them. Therefore, we can observe a fast recovery of the oxygen vacancies. The agglomeration of the vacancy clusters is thus suppressed.

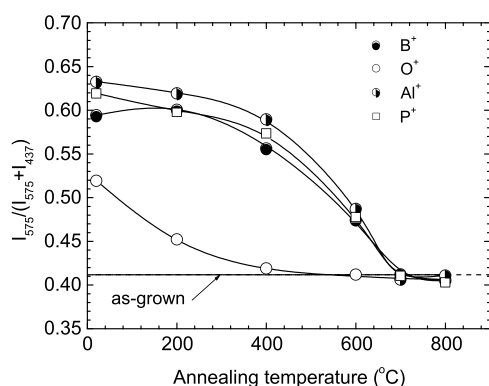

Fig. 4 Relative ratio of the integrated 575 cm^{-1} peak intensity to the sum of the 437 cm^{-1} and 575 cm^{-1} peaks as a function of annealing temperature for the implanted ZnO.

4 Conclusion Vacancy defects induced by B^+, O^+, Al^+, and P^+ ion implantation are observed by positron annihilation measurements. The annealing process for these vacancies show strong dependence on the ion species. It is suggested that the B^+ and Al^+ ions might have chemical stabilization effect on the oxygen vacancies, which favors the vacancy agglomeration during annealing.

Acknowledgements This work was partly supported by the National Natural Science Foundation of China under grant No. 10075037 and 10475062.

References

[1] U. Ozgur, Ya I. Alivov, C. Liu, A. Teke, M. A. Reshchikov, S. Dogan, V. Avrutin, S.-J. Cho, and H. Morkoc, J. Appl. Phys. **98**, 041301 (2005).
[2] D. C. Look, D. C. Reynolds, C. W. Litton, R. L. Jones, D. B. Eason, and G. Cantwell, Appl. Phys. Lett. **81**, 1830 (2002).
[3] S. O. Kucheyev, J. S. Williams, C. Jagadish, J. Zou, C. Evans, A. J. Nelson, and A. V. Hamza, Phys. Rev. B **67**, 094115 (2003).
[4] Z. Q. Chen, S. J. Wang, M. Maekawa, A. Kawasuso, H. Naramoto, X. L. Yuan, and T. Sekiguchi, Phys. Rev. B **75**, 245206 (2007).
[5] M. Tzolov, U. N. Tzenov, D. Dimova-Malinovska, M. Kalitzova, C. Pizzuto, G. Vitali, G. Zollo, and I. Ivanov, Thin Solid Films, **379**, 28 (2000).
[6] L. S. Vlasenko and G. D. Watkins, Phys. Rev. B **71**, 125210 (2005).
[7] D. R. Lide (Ed.), CRC Handbook of Chemistry and Physics, 81st ed. (CRC, Boca Raton, FL, 2000).

 © 2007 WILEY-VCH Verlag GmbH & Co. KGaA, Weinheim